Journal of Fluids and Structures (2002) **16**(1), 15–29
doi:10.1006/jfls.2001.0410, available online at http://www.idealibrary.com on IDEAL®

BY-PASS MECHANISM OF TRANSITION TO TURBULENCE

T. K. Sengupta†, M. Chattopadhyay, Z. Y. Wang and K. S. Yeo

Department of Mechanical Engineering, National University of Singapore Singapore 119 260, Singapore

(Received 17 January 2000, and in final form 10 April 2001)

The by-pass mechanism of transition for a wall-bounded shear layer is explained for the case when an infinite row of convecting vortices migrate over a boundary layer at a specific speed range. Such a mechanism is important for noisy flows over bluff bodies, flows inside turbomachinery and flows over helicopter rotor blades. By solving the Navier–Stokes equation, it is shown that this by-pass transition is a consequence of vortices migrating at convection speeds that are significantly lower than the free-stream speed. This situation is commonly found in flows that are affected by the presence of periodic wakes. Whenever the speed of migrating vortices is in a certain critical range, there is a local instability of the underlying shear layer with a very high-growth rate as compared to the growth of pure Tollmien–Schlichting waves created by wall excitation. The above interpretation is supported by solving the linearized and full Navier–Stokes equation for disturbance quantities under the parallel flow approximation in two dimensions. Various ramifications of such a by-pass route of transition are discussed in this paper.

1. INTRODUCTION

The study of transition due to convecting disturbances outside a shear layer is very important in understanding the effects of free-stream turbulence in triggering transition in shear layers over bluff bodies. It is also very important for flows in turbomachinery and rotor wing aerodynamics, where unsteady wakes from the previous stages (blades) affect the flow over the downstream stages (blades) in triggering violent transition. Above all, such a basic mechanism of transition provides an important insight into vorticity dynamics of unsteady aerodynamics.

It is well established that weak convecting vortices mutually interact with each other via Biot–Savart interactions and travel with free-stream speed. For such a disturbance field, Sengupta *et al.* (1999) showed that the response field in a boundary layer consists of a highly damped solution beneath each vortex. However, as time progresses, this solution disperses and creates response at smaller scales. This is the key to the length-scale conversion mechanism for subsequent formation of Tollmien–Schlichting (TS) waves downstream.

However, in turbomachinery, or in flows over helicopter rotor blades, it is seen that the flow in subsequent stages or blades is strongly affected by vortices that propagate at a speed lower than the free stream. For example, the experimental data and their correlation in Schlichting (1979) reveals that the far wake of a single bluff body convects at 14% of the free-stream speed. This convection speed is expected to be different in the near wake and when multiple vortices are present.

† On leave from Department of Aerospace Engineering, IIT Kanpur, India.

0889–9746/02/010015 + 15 $35.00/0

A zero pressure gradient two-dimensional boundary layer, excited by a localized, moderate frequency disturbance source inside the shear layer, displays short wavelength TS waves (Schubauer & Skramstad 1947). Gaster (1965) formulated this as a receptivity problem, with the excitation source strictly located at the wall. The corresponding full time-dependent problem was solved in Sengupta *et al.* (1994). The receptivity of this excitation is direct, because for a given value of the circular frequency, the wavenumber eigenvalue fixes the space dependence. The eigenvalues in the vicinity of the origin of the wavenumber plane constitute the asymptotic solution of the linearized Navier–Stokes equation. Apart from this asymptotic component, there is also the local solution, as discussed in Sengupta *et al.* (1994).

The receptivity to disturbances outside the shear layer is not well understood as compared to disturbances inside the shear layer. The state of the art is best revealed from the question raised in Wu *et al.* (1999) in this context: *do perturbations in the boundary layer emanate from an upstream edge or inlet and grow within the boundary layer, or are internal disturbances induced directly by external disturbances that move above the layer?* Wu *et al.* (1999) have performed the DNS of a spatially developing shear layer over a flat plate subjected to disturbances imposed by wakes entering the computational domain periodically. As the impinging wakes are released just outside the shear layer with a downward component of velocity, the associated vortices eventually enter the shear layer. This exercise was undertaken to explain the experimental results of Liu & Rodi (1991), where flow transition in turbomachines was modeled by rotating a cylinder in a circular trajectory ahead of a flat plate. The cylinder wake thus passed periodically over the flat-plate shear layer. The major findings in Wu *et al.* (1999) include the appearance of *longitudinal puffs during an initial receptivity stage, selective intensification of the puffs by a localized instability* and the generated turbulent spots *having the vague appearance of an arrowhead pointing upstream.* In the present research, the complementary problem of receptivity of a shear layer to disturbances that always remain outside the shear layer is investigated. Since the vortices are positioned far from the wall, the imposed disturbances are expected to be small. Therefore, an analysis based on the solution of linearized Navier–Stokes equation is investigated first for a parallel shear layer. To account for the growth of the shear layer, the full Navier–Stokes equation for disturbance quantities is also solved. Hunt & Durbin (1999) have discussed this as a perturbation problem, where one vortical layer interacts with another vortical layer. However, this is not treated as a problem of flow instability. Hunt & Durbin (1999) have presented some results when the interaction is weaker and the layers are sheltered from each other by large normal distances.

In Sengupta *et al.* (1997) and Sengupta & Nair (1997), the stability and receptivity aspect of free-stream excitation was considered from first principles. The existence of eigenvalues in the left-half of the wavenumber plane was established for the first time for a zero pressure gradient boundary layer, and the physical implications with respect to free-stream excitation were discussed. It was reported that these eigenvalues on the left-half plane can support free-stream excitation and they travel upstream *with respect to the disturbance sources.* In Sengupta *et al.* (1997), the upstream and downstream propagating disturbances were distinguished by their group velocity. Other properties of the upstream propagating modes revealed that these are highly stable for a zero pressure gradient boundary layer and do not lead to transition by their growth via a linear mechanism. The reason that these upstream propagating modes remained undetected is due to the fact that in traditional stability analyses, one tracks eigensolutions that satisfy homogeneous boundary conditions. In the general context of receptivity, inhomogeneous boundary conditions are natural and they lead to the discovery of a new class of waves for free-stream excitation (Sengupta & Nair 1997). It is to be emphasized that although these modes are upstream propagating *with*

respect to the source of disturbances in the free stream, in the laboratory frame, the disturbances would still propagate downstream for the parameters of the present exercise and those used in Wu *et al.* (1999). For the free-stream turbulence problem, Lieb *et al.* (1999) solved the linearized unsteady boundary layer equations, and reported finding the Klebanoff mode. However, Lieb *et al.* (1999) noted that the solution amplitudes do not reach the levels found in the experiments. It is not immediately apparent in view of the presence of upstream propagating modes, as to how an elliptic problem can be formulated as a parabolic problem.

Wu (1999) discusses the main issue in a free-stream acoustic excitation problem as one of deciphering the mechanism by which long-wavelength external disturbances become internalized as short-wavelength TS waves. In applying the triple deck theory to explain this scale conversion, one requires either some form of surface inhomogeneity or mean flow distortion (Lieb *et al.* 1999). However, Kendall (1990), through his experiments on jet-induced free-stream turbulence, has provided direct evidence of TS waves and wave packets on a nominally flat-plate boundary layer.

In this paper, the excitation of a flat-plate shear layer by convective vortical disturbance sources outside the shear layer is investigated, and a new linear instability mechanism identified. It is shown that the instability and its spectacular growth are directly related to vorticity dynamics. The organization of the paper is as follows. In the next section, the problem is formulated. This is followed by a brief discussion on the numerical method used in obtaining the primary and disturbance flow field in Section 3. In Section 4, the results are presented and discussed. Finally, in Section 5, we provide concluding remarks.

2. FORMULATION

The sketch of the problem under consideration is shown in Figure 1. An infinite array of vortices convect at a constant height Y over the flat plate and the separation distance between vortices is a. The vortices do not disperse and interact with each other as they move downstream. If these vortices convect with a constant speed, c, then the presence of the wall gives rise to the image vortex system depicted in the figure. The induced velocity components due to the total vortex system at an arbitrary point (x, y) is given by

$$u_\infty = \frac{\Gamma}{2aD} \sinh\left(\frac{2\pi Y}{a}\right) \left\{ \sin^2\left(\frac{\pi \bar{x}}{a}\right) \cosh\left(\frac{2\pi y}{a}\right) - \sinh\left(\frac{\pi}{a}(y - Y)\right) \sinh\left(\frac{\pi}{a}(y + Y)\right) \right\}, \tag{1a}$$

$$v_\infty = \frac{\Gamma}{4aD} \sinh\left(\frac{2\pi Y}{a}\right) \sin\left(\frac{2\pi \bar{x}}{a}\right) \sinh\left(\frac{2\pi y}{a}\right), \tag{1b}$$

where

$$D = \left\{ \sin^2\left(\frac{\pi \bar{x}}{a}\right) \cosh\left(\frac{2\pi y}{a}\right) - \sinh\left(\frac{\pi}{a}(y - Y)\right) \sinh\left(\frac{\pi}{a}(y + Y)\right) \right\}^2 + \left\{ \frac{1}{2} \sin\left(\frac{2\pi \bar{x}}{a}\right) \sinh\frac{2\pi y}{a} \right\}^2$$

and $\bar{x} = x - ct$.

The receptivity to this disturbance field is calculated. The u_∞ and v_∞ velocity components are plotted in Figure 2(a, b) over a single vortex spacing.

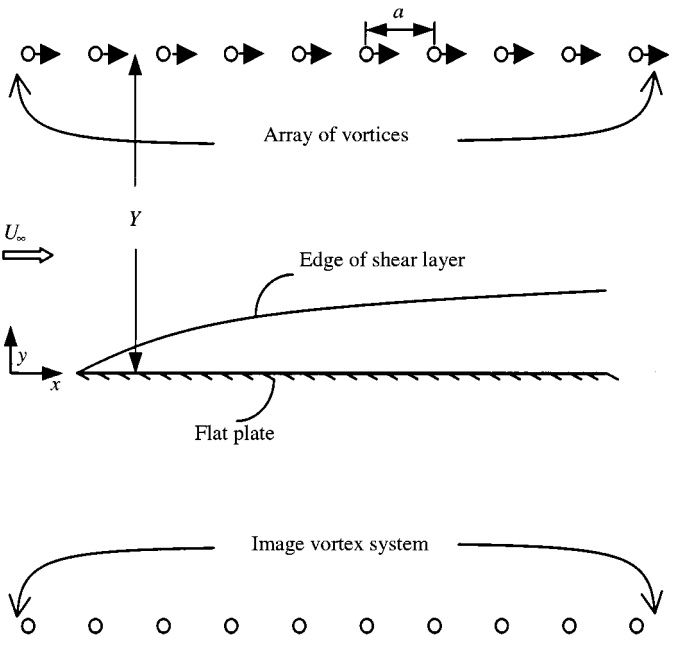

Figure 1. The physical arrangement for the convecting vortices problem.

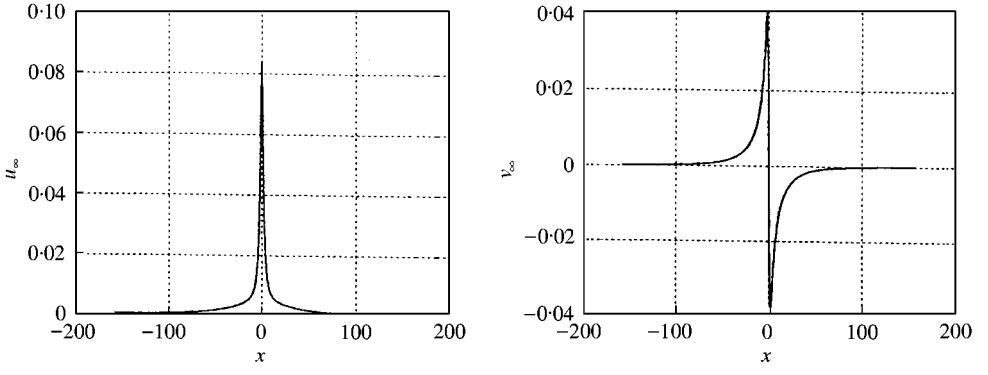

Figure 2. The imposed velocity disturbance at the free-stream boundary by the periodic train of vortices travelling at free-stream speed. The disturbance velocity components are shown for one period only for $Y = 18\delta^*$; $a = 100\pi\delta^*$ and calculated at $y = 16\delta^*$.

For the evaluation of the linearized response, the disturbance field is represented by the disturbance stream function,

$$\Psi(x, y, t) = \frac{1}{2\pi} \int_{\mathrm{Br}} \Phi(y, \alpha, \omega_0)\, \mathrm{e}^{\mathrm{i}(\alpha x - \omega_0 t)}\, \mathrm{d}\alpha \tag{2}$$

where Br is the appropriate Bromwich contour in its strip of absolute convergence (Sengupta *et al.* 1994). To fix the Bromwich contour, the group velocity of each eigenvalue is needed. The Bromwich contour is drawn in such a way that the downstream- and upstream-mode eigenvalues reside on either side of the contour. While this is the general principle for

fixing the Bromwich contour, it is a difficult undertaking because in a general excitation problem, one does not know *a priori* the number and location of all the eigenvalues. What is hoped is that the most significant eigenvalues are located and the corresponding contour is indented around these, to retain the overall correct direction of propagation of disturbances. In the present case, this effort is reduced because the Navier–Stokes simulation in the physical plane provides guidance in choosing the contour. The response given by equation (2) corresponds to the signal problem. The response of the system is at the same imposed time scale, represented by ω_0, which in turn is fixed by the spacing a and the phase speed c. Corresponding to the above disturbance stream-function, the disturbance velocity components are given by

$$u(x, y, t) = \frac{1}{2\pi} \int_{\mathrm{Br}} \Phi'(y; \alpha, \omega_0)\, \mathrm{e}^{\mathrm{i}(\alpha x - \omega_0 t)}\, \mathrm{d}\alpha, \tag{3a}$$

$$v(x, y, t) = -\frac{1}{2\pi} \int_{\mathrm{Br}} \Phi(y; \alpha, \omega_0)\, -\mathrm{i}\alpha\, \mathrm{e}^{\mathrm{i}(\alpha x - \omega_0 t)}\, \mathrm{d}\alpha. \tag{3b}$$

In the following, a prime will be used to indicate differentiation with respect to y.

The bilateral Laplace transform, Φ, in equation (2) is governed by the Orr–Sommerfeld equation, which is the spectral representation of the linearized Navier–Stokes equation under the parallel flow approximation given by

$$\Phi^{\mathrm{iv}} - 2\alpha^2 \Phi'' + \alpha^4 \Phi = \mathrm{i}\mathscr{R}e\{(\alpha U - \omega_0)(\Phi'' - \alpha^2 \Phi) - \alpha U'' \Phi\}. \tag{4}$$

The parallel mean flow $U(y)$ defines the shear layer whose displacement thickness δ^* is used to define the Reynolds number. As already noted, the prime denotes a derivative with respect to y. Equation (4) has four fundamental solutions, i.e.

$$\Phi = a_1\phi_1 + a_2\phi_2 + a_3\phi_3 + a_4\phi_4. \tag{4a}$$

These four independent fundamental solutions can be selected with the following free-stream behaviour: as $y \to \infty$ in the free stream:

$$\phi_{1\infty} = \mathrm{e}^{-\alpha y}; \quad \phi_{2\infty} = \mathrm{e}^{\alpha y}; \quad \phi_{3\infty} = \mathrm{e}^{-py}; \quad \phi_{4\infty} = \mathrm{e}^{py} \tag{4b}$$

where $p = \sqrt{\alpha^2 + \mathrm{i}\,\mathscr{R}e(\alpha - \omega_0)}$. The additional subscript '∞' in equation (4b) denotes that they are evaluated at the free stream. Now, if the real part of α and p are positive, then the first and third fundamental solutions decay with y and would be used to solve the wall- excitation problem. So, the combination of these two modes will be referred to as the wall- mode (Φ_I). Similarly, the second and fourth fundamental solutions increase with y and should be retained for finite disturbances at the free stream. Hence, a combination of these two modes will be referred to as the free-stream mode (Φ_{II}) in future discussions.

Since one has to solve equation (4) for the bilateral Laplace transform, the boundary conditions at the free stream given by equations (1) are transformed to their spectral representations, Φ_∞ and Φ'_∞. As the free-stream excitation is an even function for the streamwise component, the imaginary part of Φ'_∞ is identically zero. Also, as the wall normal component of the excitation velocity is an odd function, the imaginary part of Φ_∞ will be identically zero. The nonzero values of Φ_∞ and Φ'_∞ are shown in Figure 3. The calculations shown here are for $a = 100\pi\delta^*$ and $Y = 18\delta^*$. The other boundary conditions required to solve equation (4) are the homogeneous boundary conditions at the wall.

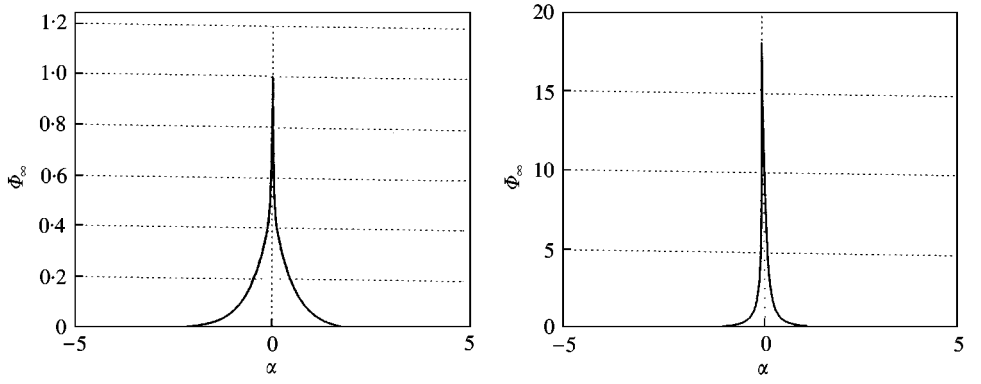

Figure 3. The bilateral Laplace transform of imposed velocity disturbance components shown in Figure 2.

3. NUMERICAL METHOD

To solve the Orr–Sommerfeld equation, one requires information on the mean flow. For a zero pressure gradient boundary layer, this is a similar profile given by the solution of the Blasius equation. Both the Blasius equation and the Orr–Sommerfeld equation are solved by a global finite-difference based generalized differential quadrature (GDQ) given by Shu & Chew (1998). By collocating the equations at the zeros of the Chebyshev polynomial, a method equivalent to the customary Chebyshev collocation is obtained. The Orr–Sommerfeld equation constitutes a boundary value problem and requires inversion of the coefficient matrix. We have used the Gauss method for this purpose.

For the vortex spacing of $a = 100\pi\delta^*$, the fundamental wavenumber (α_0) is equal to 0·02. As the fluid-dynamical system is subjected to an excitation that is periodic in space with the fundamental wavenumber as given above, the linear response of the system consists of all possible harmonics of this fundamental. In the physical plane, one would therefore observe response fields as packets whose size is given by the above fundamental wavenumber, and any instability will be associated with its higher harmonics. For a zero pressure gradient boundary layer, the shear layer is stable linearly for the above fundamental wavenumber. Thus, the packets will not grow via linear instability as they propagate downstream, while the disturbance can grow inside individual packets as it propagates downstream, corresponding to the linear instability of higher harmonics. This is precisely what Kendall (1990) had observed in his experiments, namely the simultaneous presence of wave packets with TS waves embedded in them.

Two aspects of this problem need to be emphasized. Firstly, the excitation is not monochromatic but covers a band of frequencies. This is the fundamental difference between free-stream excitation by convecting vortices and the vibrating-ribbon excitation at a fixed frequency of Schubauer & Skramstad (1947). If nonlinearity is important and one solves the full Navier–Stokes equation for the disturbance quantities, then the wave packets can grow as they propagate downstream, while the growing disturbance inside the packet can saturate in amplitude. Therefore, the solution of the Navier–Stokes equation will provide vital information about the role of nonlinearity for the problem considered. Direct simulation by the Navier–Stokes equations is also carried out.

The Navier–Stokes equation in the present study for perturbation quantities in the standard stream-function vorticity formulation are given below by

$$\frac{\partial\omega}{\partial t} + \frac{\partial}{\partial x}(u\omega + u_b\omega + u\omega_b) + \frac{\partial}{\partial y}(v\omega + v_b\omega + v\omega_b) = \frac{1}{\mathrm{Re}_1}\left(\frac{\partial^2\omega}{\partial x^2} + \frac{\partial^2\omega}{\partial y^2}\right), \tag{5}$$

$$\frac{\partial^2\psi}{\partial x^2} + \frac{\partial^2\psi}{\partial y^2} = -\omega, \tag{6}$$

where u_b, v_b and ω_b are the undisturbed base flow solution for the flat-plate boundary layer flow as given by the Blasius similarity solution. Re_1 is the Reynolds number based on the free-stream velocity, the displacement thickness at the in-flow and the kinematic viscosity. To resolve the flow gradient near the wall, the above equation is solved in a stretched coordinate system via the transformation

$$x = \xi, \qquad y = y(\eta). \tag{7}$$

In solving the equation in the transformed plane (ξ, η), the following stretching function is used in the direction normal to the wall:

$$y(\eta) = \frac{y_{\max}\sigma\eta}{\eta_{\max}\sigma + y_{\max}(\eta_{\max} - \eta)}, \tag{8}$$

where $y_{\max}$ is the height of the domain in the physical plane and $\eta_{\max}$ is the corresponding height in the computational plane; σ is a constant that can be adjusted to cluster the points near the wall.

At the in-flow boundary and on top of the computational domain, the analytical solution for the disturbance velocity is calculated in accordance with equation (1a, b). On the flat plate, the no-slip condition simultaneously provides a Dirichlet boundary condition for the stream function and the wall vorticity at every instant.

In order to eliminate the reflection of waves from the out-flow boundary, the buffer domain technique, as developed by Liu & Liu (1984), is used. The buffer domain is a narrow strip of the computational domain adjacent to the out-flow boundary. A continuous buffer function $b(\xi)$ is introduced; which has a value of 1·0 in the main computational domain, but which decreases monotonically in the buffer domain from 1·0 to 0·0 at the out-flow boundary. To treat growing or unstable modes, a second buffer function $b_{\mathrm{Re}}(\xi)$ is used to gradually reduce the Reynolds number in the buffer domain to a value below the critical Reynolds number.

Thus, the transformed governing equations in the computational (ξ, η) plane are

$$\frac{\partial\omega}{\partial t} + \frac{\partial}{\partial\xi}(u\omega + u_b\omega + u\omega_b) + \frac{1}{y_\eta}\frac{\partial}{\partial\eta}(v\omega + v_b\omega + v\omega_b)$$
$$= \frac{b_{\mathrm{Re}}}{\mathrm{Re}_1}\left(b\frac{\partial^2\omega}{\partial\xi^2} + \frac{\partial^2\omega}{\partial\eta^2}\frac{1}{y_\eta^2} + \eta_{yy}\frac{\partial\omega}{\partial\eta}\right), \tag{9}$$

$$b\frac{\partial^2\psi}{\partial\xi^2} + \frac{\partial^2\psi}{\partial\eta^2}\frac{1}{y_\eta^2} + \eta_{yy}\frac{\partial\psi}{\partial\eta} = \omega. \tag{10}$$

The buffer function of Liu & Liu (1984) is adopted here. At the outflow of buffer domain, the traditional method of extrapolation based on $\partial^2\psi/\partial\xi^2 = \partial^2\omega/\partial\xi^2 = 0$ is applied to ψ and ω.

4. RESULTS AND DISCUSSION

We begin by considering the solutions of the linearized Navier–Stokes equation for a locally parallel boundary layer. For this purpose, the Orr–Sommerfeld equation given by equation (4) is solved at 4096 equally spaced values of wavenumber along the real α-axis between $-\alpha_{\max}$ to $+\alpha_{\max}$ which constitutes the Bromwich contour. The case being considered has

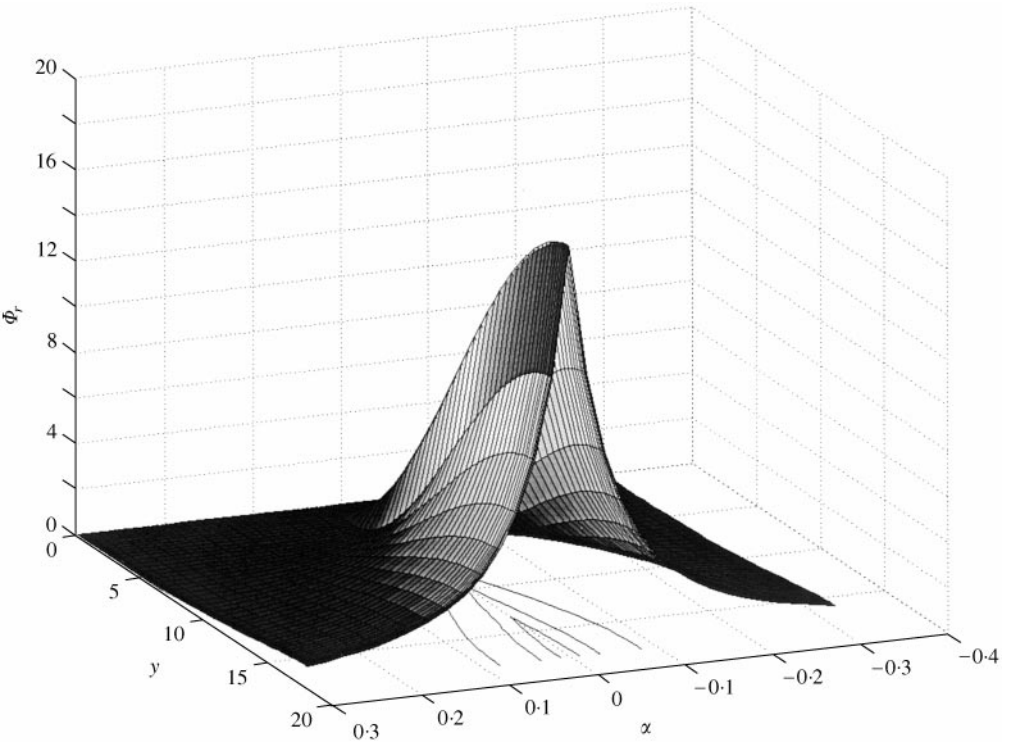

Figure 4. The perspective plot of Φ_r in the y versus α plane for the case of Figure 2, for a parallel boundary layer with Re = 1000 based on displacement thickness.

Re = 1000 and phase speed $c = U_\infty$; and the solution of the Orr–Sommerfeld equation utilizes 55 Chebyshev collocation points in the y-direction. For the chosen parameters, the evolving wave is found to be heavily damped. This suggests that the eigenvalues of all the contributing modes possess negative imaginary part. This allows us to choose the Bromwich contour along the real α-axis. A value of $\alpha_{\max} = 12{\cdot}86$ is used for the computations.

For the pure convection case, i.e. when $c = U_\infty$, the excited modes are those for which the following dispersion relation must be satisfied:

$$\alpha_n = n\omega_0, \tag{11}$$

where ω_0 is the fundamental circular frequency. Figure 4 shows the perspective plot of Φ_r over the (α, y) plane. Since the constituent modes are periodic in space (x − direction) and time, we may take the origin $x = 0$ to correspond to the instantaneous location of the perturbing vortex. In Figure 4, one cannot detect any peaks corresponding to either upstream or downstream propagating modes of the fundamental and higher harmonics.

Figure 5 shows the disturbance stream function as a function of x at the heights $y = 0{\cdot}0608\delta^*$ and $2{\cdot}1056\delta^*$. The response is severely damped at both heights, with monotonic decay in both downstream and upstream directions. This type of nonoscillatory response without any wavy component has been termed as the local solution in Sengupta *et al.* (1994).

The cause for the severely damped solution may be found in Figure 6, where the neutral curve is shown along with the c = constant loci in the (Re-ω_0) plane. The very existence of the $c = U_\infty$ line, far removed from the neutral curve, implies that such a convecting mode

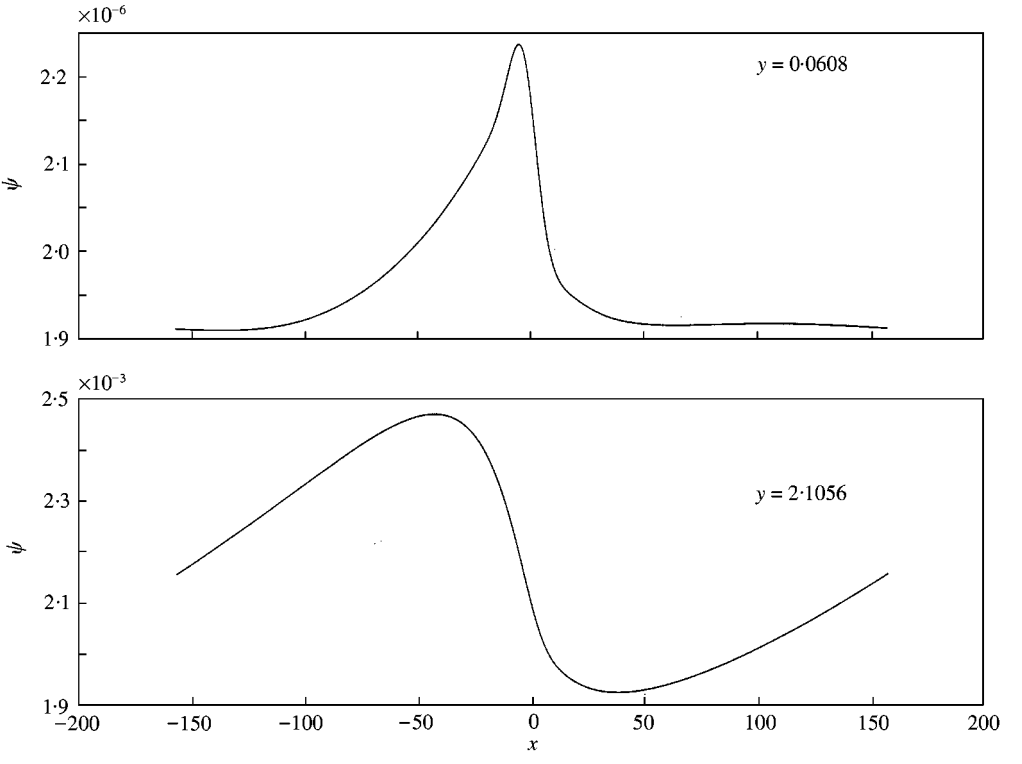

Figure 5. Disturbance stream function plotted against stream-wise distance at the indicated nondimensional heights for the case of Figure 4.

would decay very rapidly. Similarly, the upstream-propagating modes corresponding to $\omega_0 = 0{\cdot}02$ are also highly damped. The unequal damping rates of the upstream and downstream propagating modes account for the asymmetry of the solution about $x = 0$ in Figure 5. Figure 6 also indicates the possibility by which wavy or oscillatory disturbances can be generated. Of particular significance are the properties of the upstream and downstream modes with $c < U_\infty$. The real phase speed c, indicates the speed at which a free-stream disturbance would convect, and for a vortex train that does not disperse, this would be the speed of individual vortices. Figure 6 also clearly indicates that instability can be triggered if the convection speed of the vortices lies within the narrow range of $0{\cdot}26U_\infty$ to $0{\cdot}32U_\infty$. Convecting free-stream disturbances within this speed range are likely to trigger strong sustained instability, because of the high amplification rate that such modes would experience. Also, for $c > 0{\cdot}4U_\infty$, the convecting disturbances would create damped wave packets.

For such a disturbance field, the growth process is also qualitatively different as compared to the growth of disturbances that are created inside the shear layer—as done in say Schubauer & Skramstad (1947). For monochromatic wall excitation, the real frequency of the disturbance field is held fixed and the phase speed adjusts itself continuously to the local stability property of the shear layer. Contrarily, for the disturbance field generated by convecting vortices, it is the phase speed that is an invariant of the response field; while the corresponding real frequency will continuously vary, satisfying the dispersion relation given by equation (11). For free-stream excitation, the disturbance will follow a path of constant phase speed, while for localized wall excitation, this path will be along a straight line in the

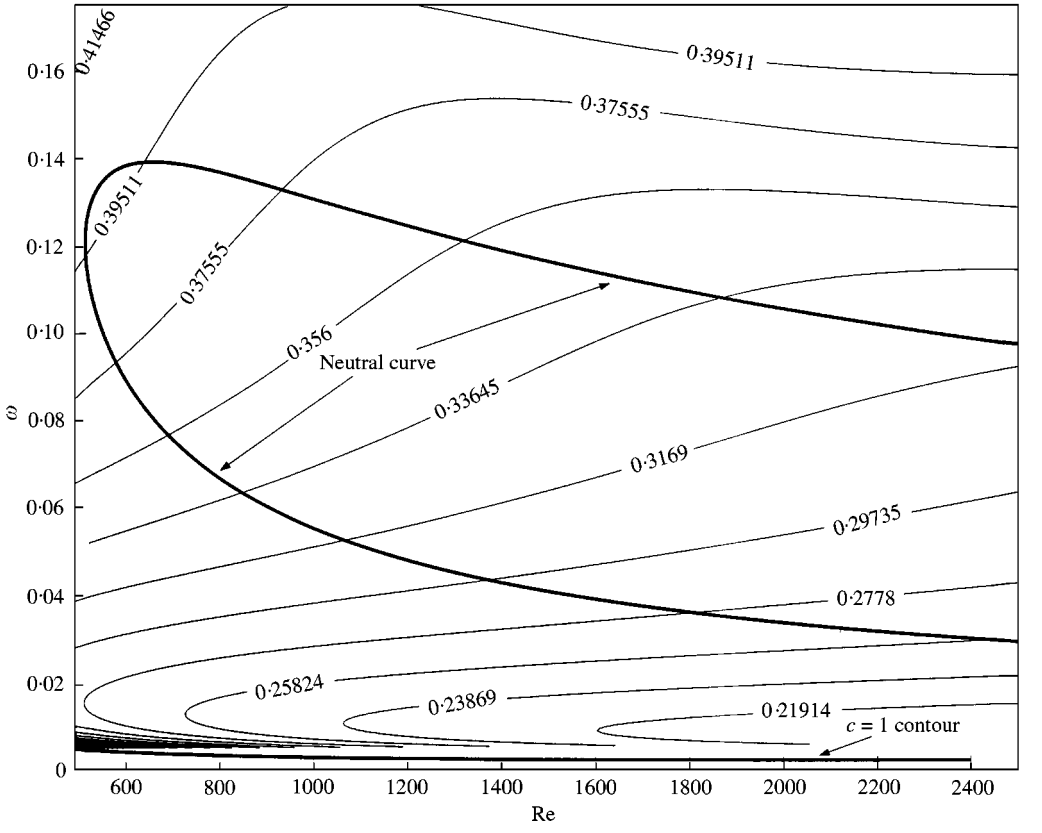

Figure 6. Stability diagram for a flat plate boundary layer showing the neutral curve superposed over c = constant disturbance propagation contours shown by thin lines. Note that the line $c = 1$ corresponds to the case of pure convection shown in Figures 4 and 5.

(Re $-$ ω_0) plane with a slope that denotes the physical frequency. Hence, if the convection speed of the vortex train is chosen to be between $0{\cdot}26U_\infty$ and $0{\cdot}32U_\infty$, then the created disturbance field inside the shear layer will suffer a sustained growth. Moreover, the rate of growth will be much higher than that for disturbances that are excited from inside the shear layer.

If one excites the shear layer by free-stream disturbances at $y = Y$, given by Φ_∞ and Φ'_∞, then it can be shown that to maintain homogeneous boundary conditions at the wall, the wall-mode should satisfy the following boundary condition for the $c = U_\infty$ case:

$$\Phi_{PC} = \Phi_I(y = 0, \alpha, \omega_0) = \mathrm{e}^{-\alpha Y}\{[\Phi_\infty(1 + \alpha Y) - \Phi'_\infty]\,\bar{\varphi}_{20} + [\Phi'_\infty - \alpha\Phi_\infty]\,\bar{\varphi}_{40}\}, \quad (12)$$

where the quantities with the additional subscript '0' on the right-hand side are the fundamental solutions as evaluated at the wall. However, when the vortices move at a speed other than the free-stream speed, the corresponding wall-mode boundary condition at the wall is given by

$$\Phi_{BP} = \Phi_I(y = 0, \alpha, \omega_0)$$

$$= \{\mathrm{e}^{-\alpha Y}[-p\Phi_\infty + \Phi'_\infty]\,\varphi_{20} - \mathrm{e}^{-pY}[\Phi'_\infty - \alpha\Phi_\infty]\,\varphi_{40}\}/(p - \alpha). \quad (13)$$

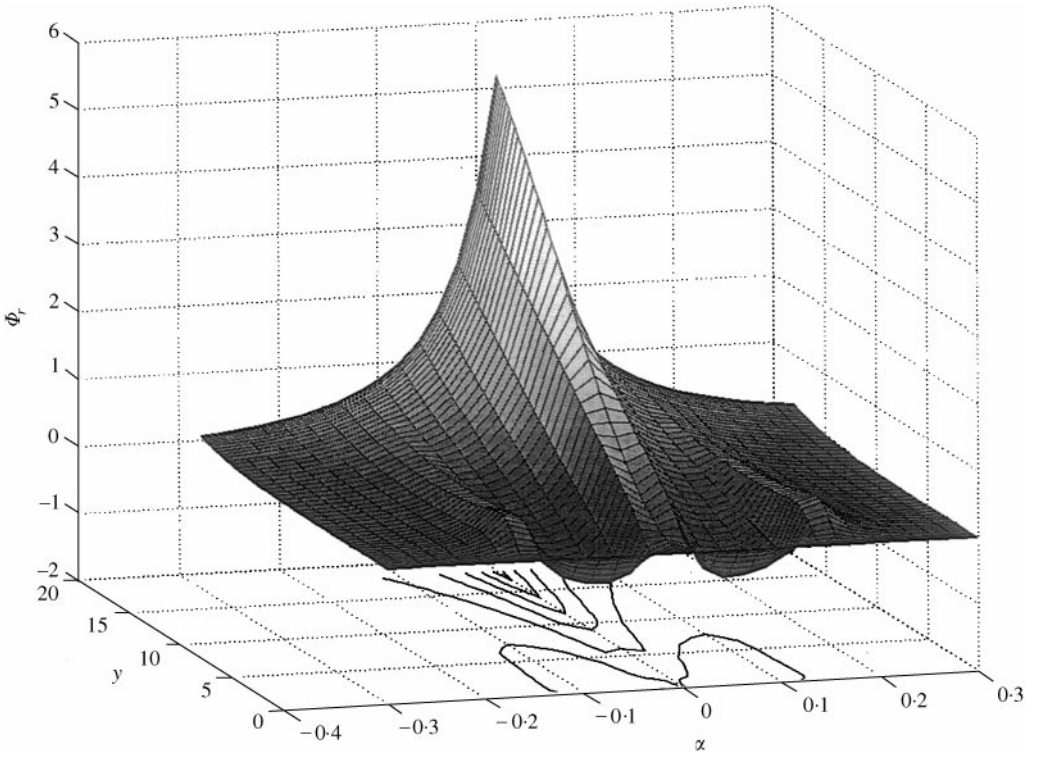

Figure 7. The perspective plot of Φ_r in the y versus α plane for the case when vortices in the freestream travel at a speed equal to $0{\cdot}3U_\infty$.

The above equations represent the equivalent wall-mode amplitudes calculated at the wall. Hence, the real parts of α and p are positive and $|p| > |\alpha|$. Also note that, for vortical free-stream disturbances, $\Phi_\infty > \Phi'_\infty$ and then

$$\frac{\Phi_{PC}}{\Phi_{BC}} = -(p-\alpha)\left\{\frac{\bar{\varphi}_{20}[\Phi_\infty(1+Y\alpha) - Y\Phi'_\infty] + \bar{\varphi}_{40}[\Phi'_\infty - \alpha\Phi_\infty]}{(\Phi'_\infty - p\Phi_\infty)\varphi_{20}}\right\}.$$

In the denominator, the term that is multiplied by e^{-pY} is neglected as compared to the retained term. This can be further simplified to

$$\frac{\Phi_{PC}}{\Phi_{BC}} = \left(\frac{\bar{\varphi}_{20}}{\varphi_{20}}\right)\left\{1 + Y\alpha - Y\frac{\Phi'_\infty}{\Phi_\infty}\right\}.$$

Hence, it becomes apparent that, for the same level of excitation at the free stream, the above ratio indicates that whether or not the TS waves are excited by free-stream vortical disturbances is determined by the height Y of the vortices over the shear layer.

Next, we consider the excitation of the parallel boundary layer by free-stream vortices convecting at $c = 0{\cdot}3U_\infty$ with $\mathrm{Re} = 1000$. In Figure 7, Φ_r is shown as a function of α and y. It is obtained by solving the Orr–Sommerfeld equation with a suitably altered dispersion relation for the free-stream disturbances. Once again, the figure is symmetric about α_i-axis. The figure clearly indicates the presence of two symmetric depressions on either side of the origin that lead to propagating disturbances within each packet. In the present exercise, the choice of Reynolds number and phase speed of the convecting vortices is such that the

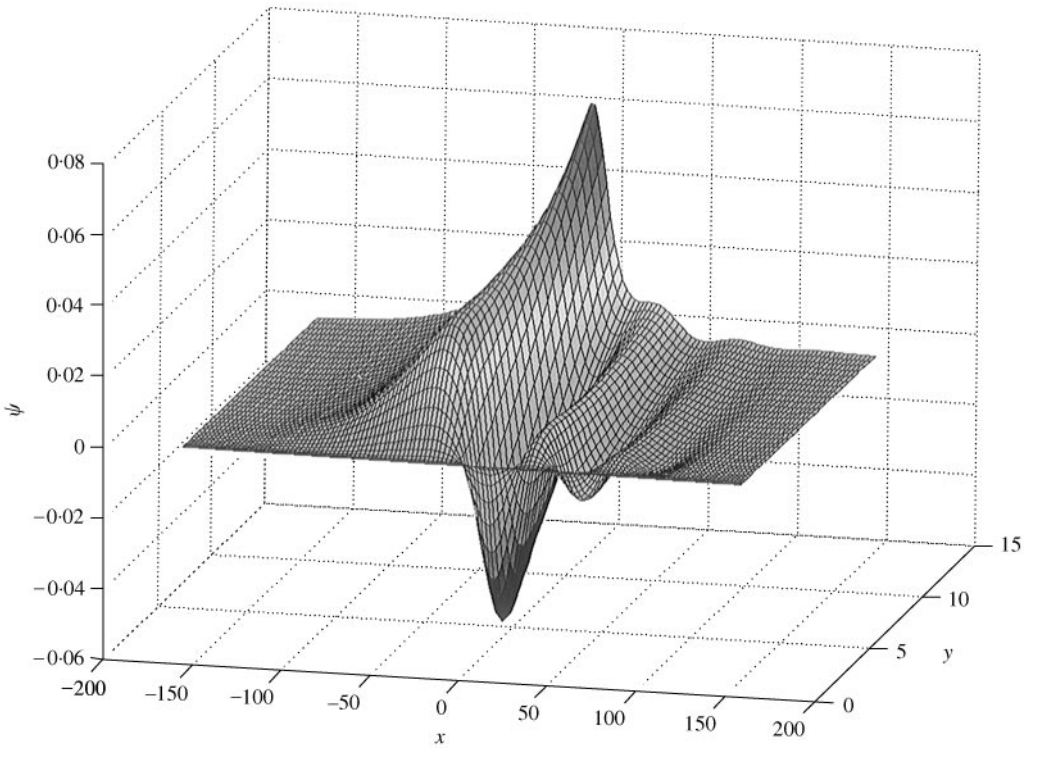

Figure 8. Disturbance stream function in the x versus y plane for the case of Figure 7.

downstream mode is lightly damped. For the choice of the Bromwich contour along the real wavenumber axis, the use of FFT is straightforward and the perturbation stream function is shown in the perspective plot in Figure 8 over the whole range of x and part of the range of y.

The result shown in Figure 8 corresponds to a parallel boundary layer. To account for the growth of the shear layer and for any nonlinearity, the Navier–Stokes equation for two-dimensional flow in the stream-function vorticity formulation is solved next. A second-order version of the GDQ procedure is used. As noted from the solution of the Orr–Sommerfeld equation in Figures 8, the parallel boundary layer exhibits damped wavy solution for $c = 0{\cdot}3U_\infty$ and $\mathrm{Re} = 1000$. However, owing to the growth of shear layer for the Navier–Stokes solution and consequent increase in the Reynolds number, the disturbances downstream can become unstable-as can be seen from Figure 6. In Figure 9, the solution of the Navier–Stokes equation for $c = U_\infty$ case is shown, and one notices only the local solution at early time. This solution disperses as time progresses while the amplitude of the disturbances decays. This dispersion of the solution is governed by the upstream propagating modes as reported in Sengupta *et al.* (1999).

Next, the case for $c = 0{\cdot}3U_\infty$ was investigated by solving the Navier–Stokes equation. One would expect to see a rapid growth of disturbances based on the preceding analysis of Figure 6. For the two-dimensional Navier–Stokes equation, the shear layer grows with downstream distance and the Reynolds number changes from $\mathrm{Re} = 165$–1900 for the chosen computational domain. The results showing the streamwise component of the disturbance velocity are given in Figure 10(a) and 10(b) for $y = 0{\cdot}3\delta^*$ and $1{\cdot}5\delta^*$, respectively. While the present results are for two-dimensional flow, similar computations have been

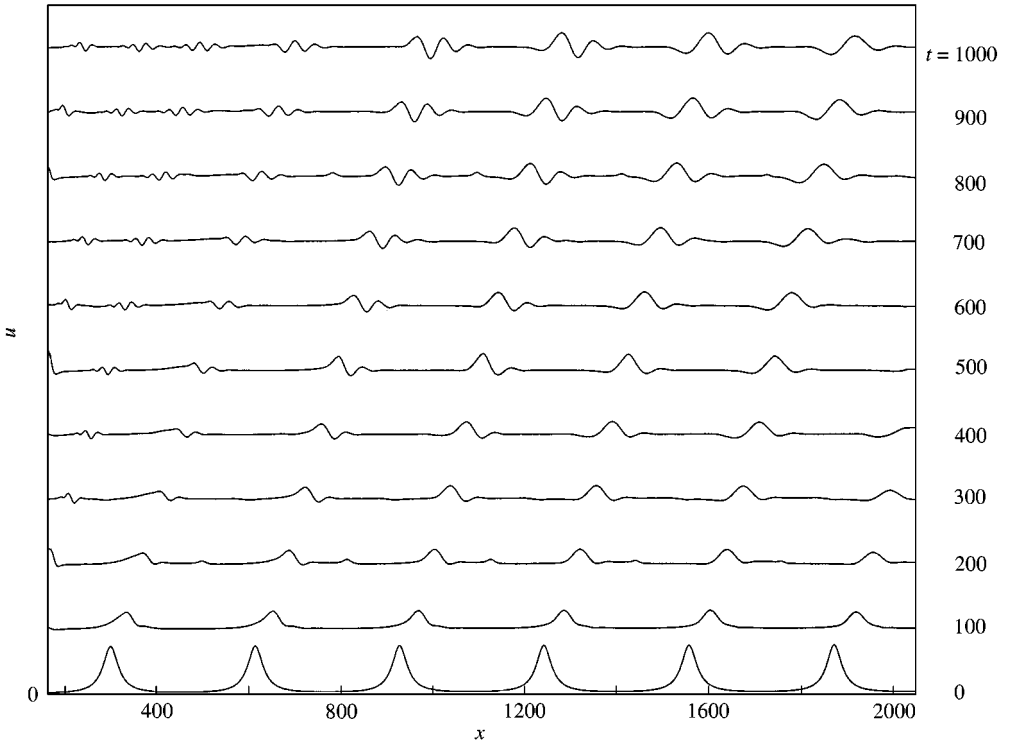

Figure 9. Streamwise disturbance velocity component evaluated at $y = 0{\cdot}3\delta^*$ for the indicated times by solving Navier–Stokes equation for disturbance quantities for the excitation field as shown in Figure 2. The x-axis corresponds to the Reynolds number based on local δ^* corresponding to zero pressure gradient similarity profile.

performed for 3-D flows by Wu *et al.* (1999) for free-stream vortices that were directed towards the plate by the imposition of a constant downward velocity at the inflow. The resultant trajectory of the vortex-induced disturbance is intuitively expected to lie in the southeast direction if the mean flow is from west to east. However, the induced disturbance field moved in the southwest direction instead, clearly indicating that the free-stream excitation causes a disturbance field that propagates upstream, as predicted by Sengupta *et al.* (1999). Wu *et al.* (1999) have also noted the existence of such local instability from their DNS. The existence of common features among the results from the 3-D DNS, 2-D DNS and solution of linearized Navier–Stokes problem is not accidental and points to the existence of a common mechanism that is seen in all the three.

While writing the final version of the paper, our attention has been drawn to experimental work performed by Kendall (1987) that was similar to the experiment performed by Liu & Rodi (1991) later. Unlike Liu & Rodi (1991), in Kendall (1987), the cylinder rotated in a circular trajectory above the plate, and the resultant excitation is in a sense qualitatively similar to the present investigations. In the experiment of Kendall (1987), the strength, location and migration speed of the vortices are, however, not controlled. But the results, indicated in figure 3 of that paper, clearly showed that a rotation speed that corresponded to $c = 0{\cdot}3U_\infty$ showed maximum receptivity, as compared to $c = 0{\cdot}23U_\infty$ and $0.5U_\infty$. Also, the hot-wire oscillograms corresponding to the circumferential speed of $0.3U_\infty$ of the rotor indicated the presence of large amplitude wave packets.

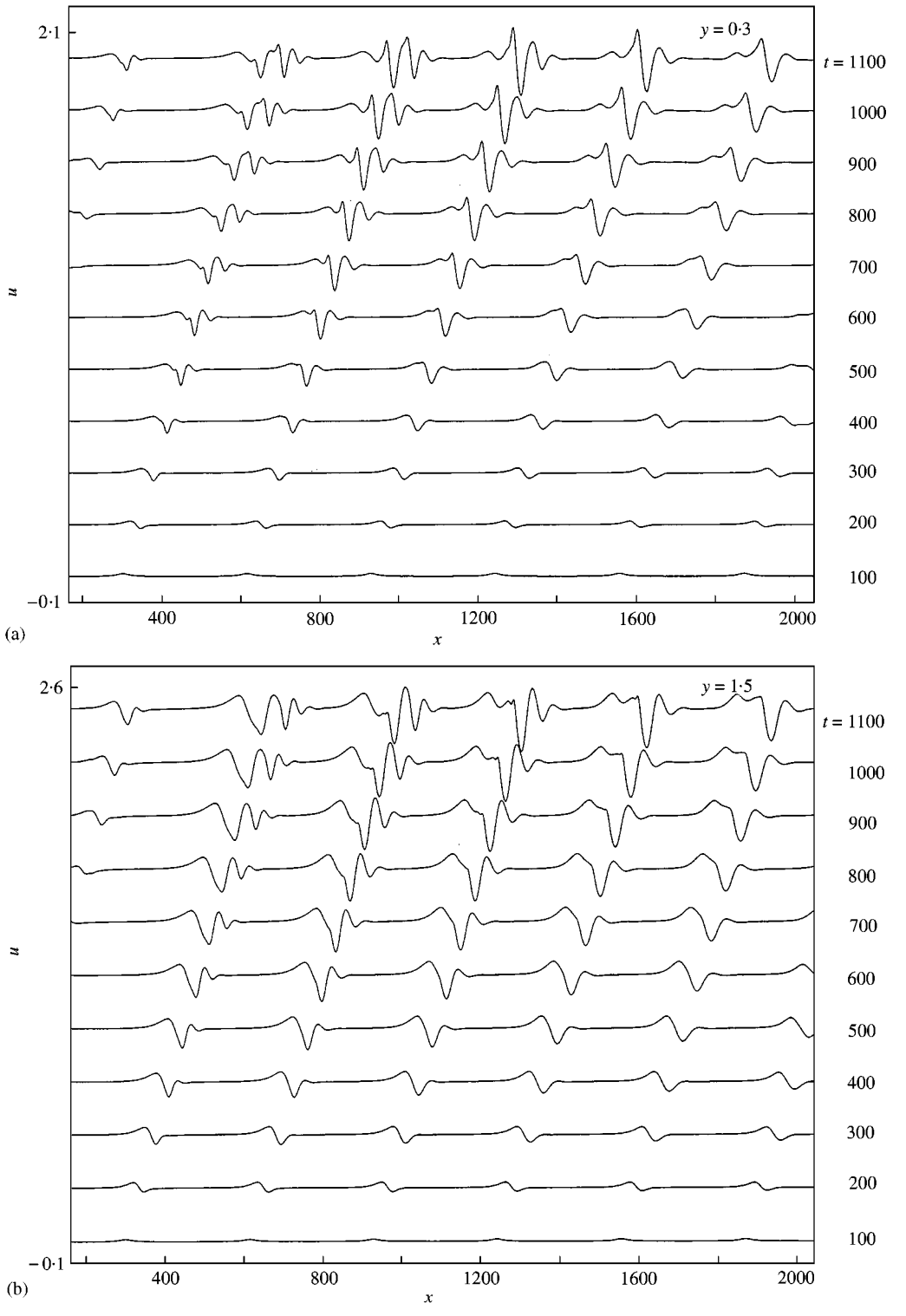

Figure 10. (a). Streamwise disturbance velocity component evaluated at $y = 0{\cdot}3\delta^*$ for the indicated times for $c = 0{\cdot}3U_\infty$, obtained from disturbance Navier–Stokes equation. (b). Streamwise disturbance velocity component at $y = 1{\cdot}5\delta^*$ for the case of $c = 0{\cdot}3U_\infty$ at indicated times, obtained as solution of the Navier–Stokes equation for perturbation quantities.

5. CONCLUDING REMARKS

The present study clearly shows that free-stream vortical excitation can give rise not only to short wavelength downstream-propagating disturbances inside the shear layer and upstream-propagating disturbances postulated in Sengupta *et al.* (1999), but also initiate very large disturbance growth within the shear layer if the propagating free-stream disturbances travel at a constant speed range that is much below the free-stream speed. The most effective speed range is seen to be between $0{\cdot}26U_\infty$ and $0{\cdot}32U_\infty$. Furthermore, such disturbance growth can be spectacularly larger than the wall-excitation case because the constant-c disturbances are able to track the most unstable local modes of the shear layer in a sustained manner. We believe that this is the by-pass transition mechanism for periodic free-stream perturbation, as in turbomachinery—although the term may have been used in different contexts by other researchers. This study also indicates that the by-pass route of transition is potentially more severe as compared to wall excitation.

ACKNOWLEDGEMENT

The authors wish to acknowledge valuable discussions with Prof. T.T. Lim during the preparation of this paper. The first author wishes to acknowledge the visiting fellowship offerred by the department of ME at NUS during the course of which this work was undertaken.

REFERENCES

GASTER, M. 1965 On the generation of spatially growing waves in a boundary layer. *Journal of Fluid Mechanics* **22,** 433–441.

HUNT, J. C. R. & DURBIN, P. A. 1999 Perturbed vortical layers and shear sheltering. *Fluid Dynamics Research* **24,** 375–404.

KENDALL, J. M. 1987 Experimental study of laminar boundary layer receptivity to a traveling pressure field. AIAA Paper 87-1257.

KENDALL, J. M. 1990 Boundary layer receptivity to freestream turbulence. AIAA paper 90-1504.

LEIB, S. J., WUNDROW, D. W. & GOLDSTEIN, M. E. 1999 Effect of free stream turbulence and other vortical disturbances on a laminar boundary layer. *Journal of Fluid Mechanics* **380,** 169–203.

LIU, Z. & LIU, C. 1994 Fourth order finite difference and multigrid methods for modeling instabilities in flat plate boundary layer-2D and 3D approaches. *Computers and Fluids* **23,** 955–982.

LIU, X. & RODI, W. 1991 Experiments on transitional boundary layers with wake induced unsteadiness. *Journal of Fluid Mechanics* **231,** 229–256.

SCHLICHTING, H. 1979 *Boundary Layer Theory*, 7th edition. New York: Mc Graw Hill.

SCHUBAUER, G. B. & SKRAMSTAD, H. K. 1947 Laminar boundary-layer oscillations and stability of laminar flow. *Journal of Aeronautical Sciences* **14**, 69–78.

SENGUPTA, T. K., BALLAV, M. & NIJHAWAN, S. 1994 Generation of Tollmien-Schlichting waves by harmonic excitation. *Physics of Fluids* **6,** 1213–1222.

SENGUPTA, T. K., NAIR, M. T. & RANA, V. 1997 Boundary layers excited by low frequency disturbances-Klebanoff mode. *Journal of Fluids & Structures* **11,** 845–853.

SENGUPTA, T. K. & NAIR, M. T. 1997 A new class of waves for Blasius boundary layer. In *Proceedings of Seventh Asian Congress of Fluid Mechanics*, Chennai, India, pp. 785–788.

SENGUPTA, T. K., WANG, Z. Y., YEO, K. S. & CHATTOPADHYAY, M. 1999 Receptivity to convected vortices-by-pass route. In *Proceedings of Eighth Asian Congress of Fluid Mechanics* (*ed. E. Cui*), Beijing, China, pp. 964–968.

SHU, C. & CHEW, Y. T. 1998 On the equivalence of generalized differential quadrature and highest order finite difference scheme. *Computer Methods in Applied Mechanics and Engineering* **155,** 249–260.

WU, X., JACOBS, R. G., HUNT, J. C. R. & DURBIN, P. A. 1999 Simulation of boundary layer transition induced by periodically passing wakes. *Journal of Fluid Mechanics* **399,** 109–153.

WU, X. 1999 Generation of Tollmien-Schlichting waves by convecting gusts interacting with sound. *Journal of Fluid Mechanics* **397,** 285–316.